Clays and Clay Minerals, Vol. 48, No. 3, 351–365, 2000.

CLAY-MINERAL AUTHIGENESIS IN THE LATE PERMIAN COAL MEASURES, BOWEN BASIN, QUEENSLAND, AUSTRALIA

I. TONGUÇ UYSAL, SUZANNE D. GOLDING, AND FRANK AUDSLEY

Department of Earth Sciences, The University of Queensland, Brisbane, Queensland 4072, Australia

Abstract—Mineralogical studies were performed on authigenic clay minerals of mudrocks, sandstones, and bentonites from 38 boreholes in the Late Permian coal measures of the Bowen Basin. Clay-mineral separations of samples from the northern Bowen Basin consist mainly of (Reichweite, R) R = 1 and R ≥ 3 interstratified illite-smectite (I-S), chlorite, and kaolinite. In the southern Bowen Basin, samples from higher stratigraphic sections are characterized by randomly ordered (R = 0) I-S mixed layers, and kaolinite and chlorite in smaller amounts. Samples from the lower sections consist of (R ≥ 3) I-S, chlorite, chlorite-rich chlorite-smectite (C-S), and laumontite.

Examination of the mineralogy and distribution of authigenic clay minerals from the Late Permian coal measures in the northern part of the Bowen Basin indicated that the presence of clay minerals is not systematically related to depth and clay occurrences do not occur regularly. These mineralogical variations of clay in volcaniclastic sediments are incompatible with thermal control. Variations in the rate of fluid flow and potassium supply owing to permeability exert major influences on clay-mineral paragenesis and the reaction of illitization. In more permeable zones (possibly faults or fracture zones), highly illitic clays with lath-shaped morphologies may have precipitated directly from potassium-rich fluids migrating from deeper parts of the basin. In addition, abundant chlorite precipitated contemporaneously with illitic clays, which may have resulted from sufficient magnesium and iron occurring in the fluids as a result of dissolution of intermediate or mafic-rock fragments. At the same time, clay paragenesis with less illitic I-S, kaolinite, and minor chlorite occurs outside the channelized zones of high fluid flow, where a diffusive-flow regime may have predominated with lower ratios of the activities of K^+ and H^+ (*i.e.*, $\alpha_{K^+}/\alpha_{H^+}$) in the solutions.

In the southern Bowen Basin, depth-related changes in the distribution of clay minerals are evident and may be indicative of thermal control on clay-mineral reactions. Zeolites are present locally in the Late Permian volcaniclastic rocks in the southern Bowen Basin, but not in the north. This is attributed to a low ratio of $\alpha_{CO_2}/\alpha_{H_2O}$ (where α = activity) and/or more saline and alkaline solutions.

Key Words—Chlorite, Clay-Mineral Distribution, Fluid Flow, Illite-Smectite, Kaolinite.

INTRODUCTION

The significance of clay minerals, particularly illite-smectite (I-S) interstratifications, as potential indicators for geothermometry has been recognized from studies of deeply buried sedimentary basins (Hower *et al.*, 1976; Hoffman and Hower, 1979; Pollastro, 1990, 1993), fossil and active hydrothermal systems (Horton, 1985; Flexser, 1991; Ylagan *et al.*, 1996), and contact-metamorphic environments (Nadeau and Reynolds, 1981; Bühmann, 1992; Esposito and Whitney, 1995). In addition, clay minerals provide important records of paleo-fluid flow and fluid chemistry during post-depositional evolution of sedimentary basins (Whitney and Northrop, 1987; Owen *et al.*, 1989). Many studies showed that in chemically open systems, temperature is not the only factor driving clay-mineral reactions, but also factors, such as pore-fluid chemistry, porosity-permeability, and residence time may affect the reaction significantly (Ramseyer and Boles, 1986; Owen *et al.*, 1989; Patrier *et al.*, 1996). For example, pore-fluid chemistry was emphasized as a critical factor in controlling clay-mineral composition in the San Juan Basin where the most highly illitized zones were attributed to reactions with saline and alkaline fluids (Owen *et al.*, 1989). In addition, an experimental study (Huang, 1992) showed that a positive correlation exists between the number of illite layers in I-S and potassium concentration of initial solutions at a constant temperature. The rate of fluid flow as related to porosity-permeability was shown to be an important factor to determine clay-mineral assemblages and to determine the extent of illitization in sedimentary basins (*e.g.*, Whitney and Northrop, 1987) and hydrothermal environments (*e.g.*, Harvey and Browne, 1991; Patrier *et al.*, 1996). Several studies showed that clay reactions are time sensitive and, at a given temperature, they may show considerable variations owing to differences in heating time (Ramseyer and Boles, 1986; Velde and Vasseur, 1992).

Subsidence and sediment accumulation in the Bowen Basin began in the Early Permian and ended during the Middle Triassic at ~235–230 million years ago (Ma) with the final contractional phase of the Hunter-Bowen Orogeny (Baker and Caritat, 1992; Fielding *et al.*, 1997). This event corresponds with maximum burial of Bowen Basin sediments to a depth of 3000–3500 m (Baker and Caritat, 1992). The orogeny is believed to be responsible for thermal maturation of the Late Permian coals in the Bowen Basin (Baker and

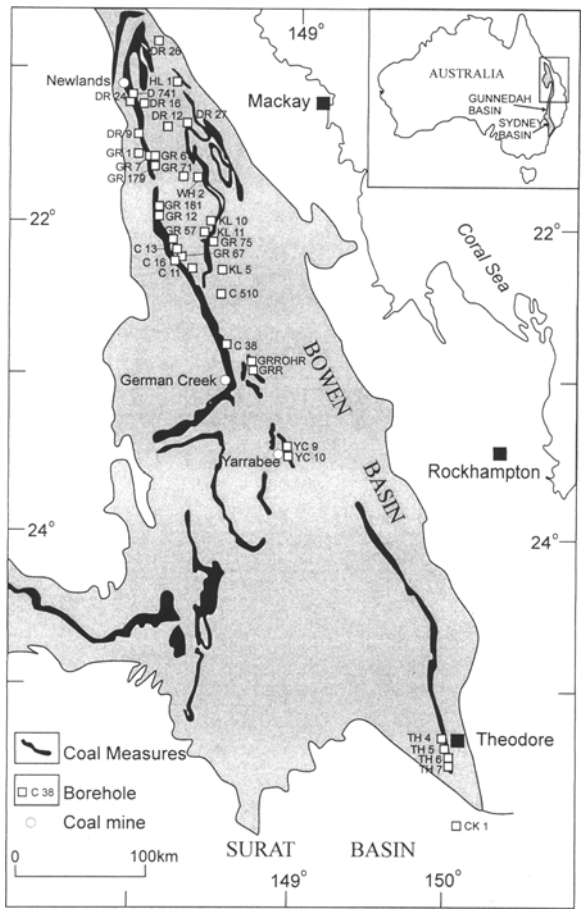

Figure 1. Map of the study area and sampling localities.

Caritat, 1992; Mallett *et al.,* 1995). Vitrinite reflectance (R_o) values in the Bowen Basin range from 0.45% R_o in the Rangal Coal Measures in the southern part of the basin to over 3.5% R_o in the Moranbah Coal Measures in the northern Bowen Basin. The Late Permian sections have significantly high reflectance gradients, which are similar to those for basins with high geothermal gradients (Uysal *et al.,* 2000a). These results and the radiometric dating of I-S suggest that organic maturation and widespread illite formation in the Bowen Basin Coal Measures occurred largely as a result of a short-lived hydrothermal event at ~210 Ma during an extensional phase rather than a result of maximum burial in the Middle Triassic (Uysal *et al.,* 2000b). In this study, we (1) document the mineralogy, texture, and distribution of authigenic clay minerals in the Late Permian Coal Measures, (2) determine the importance of fluid chemistry and rock permeability, and (3) evaluate the formation mechanism and origin of the clays.

GEOLOGIC SETTING

The Bowen Basin, located in east-central Queensland, forms the northern part of the ~2000-km long Bowen-Gunnedah-Sydney Basin System in eastern Australia (Figure 1). The northern half of the Permo-Triassic Bowen Basin is exposed and extends from Collinsville in the north southwards to ~25°S, where it is overlain by Jurassic-Cretaceous sediments of the Surat Basin. The Bowen Basin is one of the most important coal-bearing basins in the world, with reserves of ~20,000 million tons of Permian coal (Mallett *et al.,* 1995).

On the basis of stratigraphic and sedimentological studies (Fielding *et al.,* 1997), a three-phase model was proposed for the geological evolution of the Bowen Basin: (1) an Early Permian episode of extensional subsidence associated with volcanic activity; (2) an early Late Permian phase of passive thermal subsidence; and (3) a Late Permian to Middle Triassic phase of foreland thrust load-induced burial. Rocks of the early Permian successions of the extensional phase are comprised of predominantly fine-grained sedimentary rocks interlayered with mafic-dominated volcanic rocks of the Lizzie Creek Volcanics in the north and the Camboon Volcanics in the southeast (Figure 2). Following the infilling of the extensional topography, the Bowen Basin region started to subside slowly and evenly across the area, resulting in widespread marine transgression and accumulation of fine-grained marine strata (Fielding *et al.,* 1997) to form the (passive thermal-subsidence phase) Back Creek Group (Figure 2). A major change occurs in the sandstone petrology and depositional environment of the Late Permian rocks. This change resulted from the onset of thrust loading of the eastern Bowen Basin and resurgence of the volcanic arc to the east (Baker *et al.,* 1993; Fielding *et al.,* 1997). These tectonic events resulted in the rapid introduction of a first-cycle, volcanic lithic-sediment shed westward across the Bowen Basin (Baker *et al.,* 1993). Consequently, strata consisting initially of quartzitic, craton-derived sediment from the west became more uniformly volcanic lithic in composition. The Middle Permian marine strata coarsen upward into a coarse-grained non-marine clastic facies, which represents the final infilling of the marine Bowen Basin. The resulting topography established the alluvial plain systems across the region (Fielding *et al.,* 1997). The formation of the latest Permian coal measures is a response to the high-energy alluvial conditions near the basin margin, where coarse clastic sediment from the rising, volcanically active orogen accumulated westward into the basin (Fielding *et al.,* 1997). Following the final infilling of the Bowen Basin by volcanogenic sediments, uplift and thrust loading produced reddened alluvial sediments of the Rewan Group throughout the basin shortly before the Permian-Triassic boundary (Baker *et al.,* 1993). The Early Triassic structural event created uplift in both the craton to the west and the arc to the east, resulting in large amounts of coarse-grained quartzitic and dissected arc-derived sediments

https://doi.org/10.1346/CCMN.2000.0480306 Published online by Cambridge University Press

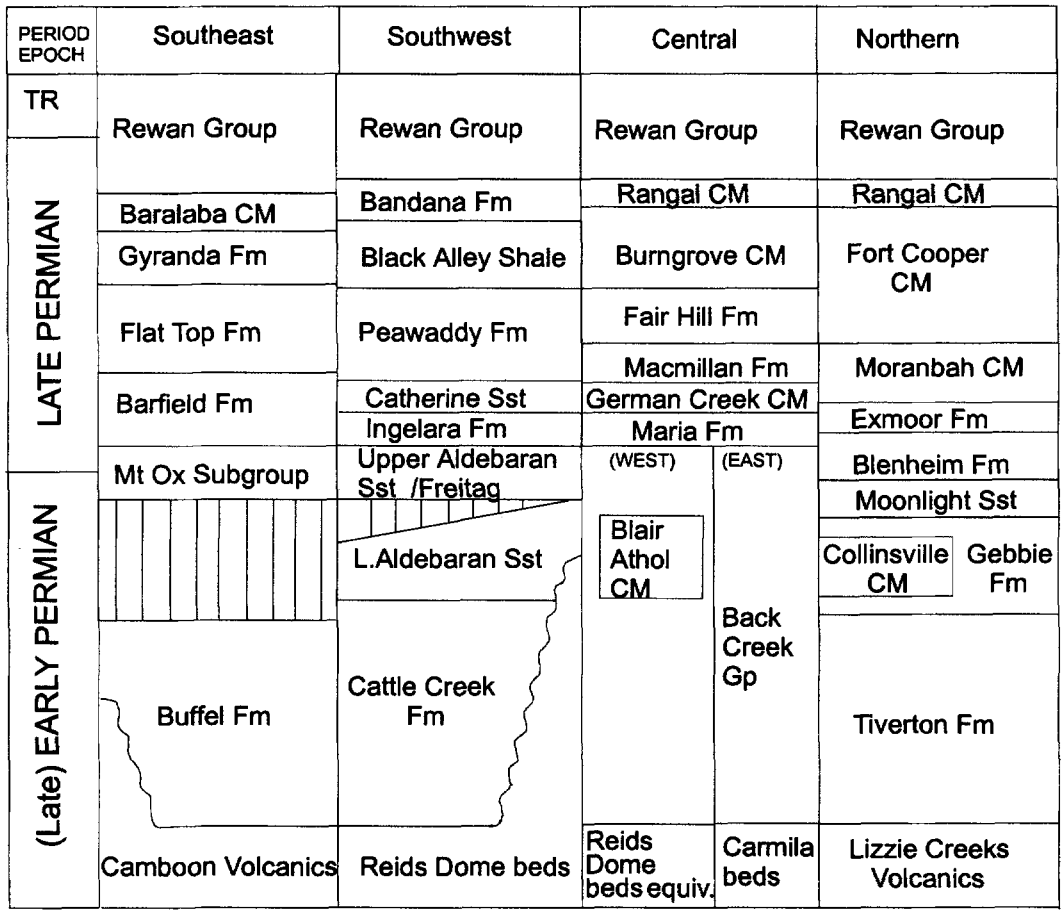

Figure 2. Lithostratigraphic correlations for the Bowen Basin (after Draper *et al.*, 1990).

into the basin during the Middle Triassic (Baker *et al.*, 1993). Sediment accumulation in the Bowen Basin terminated around 235–230 Ma as a result of thin-skinned thrust deformation of the basin during the Hunter-Bowen Orogeny, followed by erosion of the basin fill (Fielding *et al.*, 1997). The Late Permian to Middle Triassic crustal contraction (Hunter-Bowen event) was followed by an episode of crustal extension affecting eastern Australia in the Late Triassic (Fielding *et al.*, 1997). Middle Cretaceous transtension to extension was associated with widespread intrusions in the northern part of the Bowen Basin (Golding *et al.*, 1999).

ANALYTICAL PROCEDURES

A total of 256 samples of mudstone, siltstone, bentonite, and sandstone were examined for clay and whole-rock mineralogy. Washed core samples were reduced in size with a hammer and by hand grinding in an agate mortar. To prepare a randomly oriented grain-aggregate mount to determine whole-rock mineralogy, powders of bulk sample were back loaded into an aluminum holder.

To prepare a sample for separation of the clay-size fraction, rock chips were gently crushed to sand-size particles. Approximately 10–20 g of the bulk sample were disaggregated in 200 mL distilled water by stirring vigorously for 1–2 min. Suspensions in beakers were placed in an ultrasonic bath for 2–3 min to ensure complete disaggregation. Different clay-size fractions (<2, 2–0.8, 0.8–0.2, and <0.2 μm) were obtained by centrifugation. The decanted clay suspension was placed on a glass slide. Following the X-ray diffraction (XRD) analysis of air-dried samples, the oriented clay-aggregate mounts were placed in an ethylene-glycol atmosphere at 30–40°C overnight. After XRD patterns for these samples were made, selected slides were heated at 375–400 and 550°C for >1 h to determine the presence of I-S mixed-layer phases, chlorite, and kaolinite. These analyses were performed on a Philips PW1840 XRD unit operated at 40 kV and 25 mA at a scanning rate of 1.2 °2θ/min with CoKα radiation. Whole-rock random-powder patterns were recorded from 2 to 75 °2θ; and oriented clay-aggregate specimens from 2 to 40 °2θ in an air-dried state, after eth-

https://doi.org/10.1346/CCMN.2000.0480306 Published online by Cambridge University Press

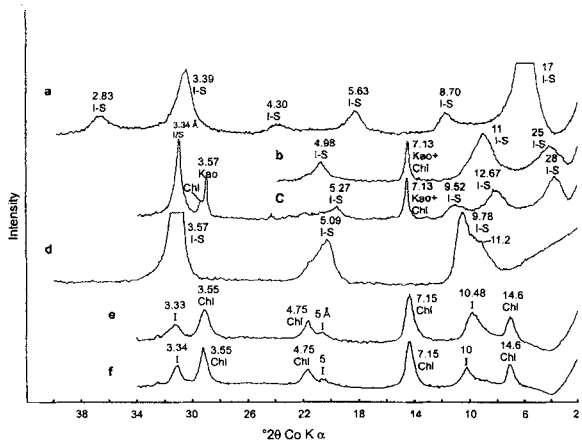

Figure 3. Representative X-ray diffraction patterns of clays from the Bowen Basin. (a) Sample TH 4-7 from the Baralaba Coal Measures from 320 m, mudstone (<0.2-μm fraction, glycolated). (b–c) Sample GRR-12 from the Rangal Coal Measures from 66 m, siltstone (<2-μm fraction, b: air-dried, c: glycolated). (d) Sample GR 71-3 from the Fort Cooper Coal Measures from 75.6 m, mudstone (<0.2-μm fraction, glycolated). (e–f) Sample DR 26-172 from the Moranbah Coal Measures from 172 m, sandstone (<2-μm fraction, e: air-dried, f: glycolated). I-S = illite-smectite mixed-layers, Kao = kaolinite, I = illite Chl = chlorite. Numbers above peaks are *d* values in Å.

ylene-glycol treatment, and for some selected samples after heating to 375 and 550°C.

To determine illite content in illite-smectite mixed-layer clays, the method of differential two-theta (Δ2θ) was used. In this method, (Moore and Reynolds, 1989), the angular difference between the 001 and 002 peaks of illite-smectite and the 002 and 003 peaks is used to estimate the percentage of illite in an illite-smectite phase. The analytical error is about ±5% but may be higher for impure samples containing discrete illite. Estimates of the relative abundance of clay minerals in different size fractions were obtained using techniques of Biscaye (1965) and Schultz (1964). Additional data, for the mineralogy of the clay and bulk-rock mineralogy by XRD are given in Uysal (1999).

Sandstone samples were examined using optical petrography (60 samples). For 22 samples, modal analyses were obtained by counting 300–400 points per thin section. Scanning electron microscopy (SEM) and energy-dispersive elemental X-ray (EDX) system using a JOEL 6400 microscope enabled characterization of 20 samples for morphology and chemical composition of the clay and carbonate minerals. For these analyses, rock chips were mounted on aluminum stubs and sputter coated with gold.

TEM examination was made with a JEOL 1210 transmission 1210 transmission electron microscope on nearly pure I-S separates from six mudstones. Clay suspensions were diluted in distilled water, disaggregated in an ultrasonic bath, and allowed to dry on carbon-coated copper grids.

RESULTS

XRD

Representative XRD data (Figure 3) give the mineralogy of the <2 and <0.2-μm fractions of mudrocks, sandstones, and bentonites. Interstratified I-S is the dominant clay mineral in most samples. Three types of I-S were observed: (1) I-S observed mostly from the Baralaba Coal Measures in the southern Bowen Basin display random (Reichweite, R = 0) I-S (note the 17-Å peak with ethylene glycolation, Figure 3a). These clays contain <55% illite layers in I-S. (2) The second type of I-S is common from the northern part of the Bowen Basin, and it is characterized by a superstructure reflection at 26–28 Å and by diffraction peaks near 9–9.5 and 13 Å after ethylene glycolation (Figure 3b and 3c). These clays are (R = 1) I-S and contain 65–85% illite layers. (3) The third type of I-S is R ≥ 3. These clays show asymmetrical peaks at ~9.8 Å, with a broad shoulder near 11 Å when glycolated. These shoulders are observed only in samples containing >85% illite layers (Figure 3d). Some illitic clays show a small change in intensity at the high-angle side of the 001 reflection after glycol treatment, indicating that only a few percent of expandable layers occur in the samples (Figure 3e and 3f). Some XRD patterns show partial R = 2 ordering which is characterized by ~18–19-Å (second order of 37-Å peak) and ~11.5–13-Å (third order) reflections of glycolated samples.

I-S is most abundant in samples of the finer clay fractions (<0.8 μm). Many samples of clay fractions of <0.2 μm, mostly from the Fort Cooper Coal Measures, consist of nearly pure I-S. In addition, clay separates in the <2-μm fraction of many bentonite samples are composed of nearly pure I-S. The XRD data show that the illite content in the interstratified clays is generally the same in both the mudrocks and the adjacent sandstones but, in some cases, the mudrocks were observed to be slightly more illitic than the adjacent sandstones. The I-S interstratified forms from the bentonites generally contain fewer illite layers than those from the interbedded mudrocks and sandstones.

Kaolinite occurs mostly in samples from the Rangal Coal Measures (Figure 4). Rarely, kaolinite comprises the bulk of the clay-mineral fraction in the shallowest part of the wells in the Rangal Coal Measures. It is less abundant in the Moranbah Coal Measures and especially in the Fort Cooper Coal Measures (Figure 4). Kaolinite is usually detected in the coarser size fractions (>0.8 μm) of the samples in which I-S contains ≤80% illite layers. Kaolinite is not present with highly illitic (R ≥ 3) I-S.

https://doi.org/10.1346/CCMN.2000.0480306 Published online by Cambridge University Press

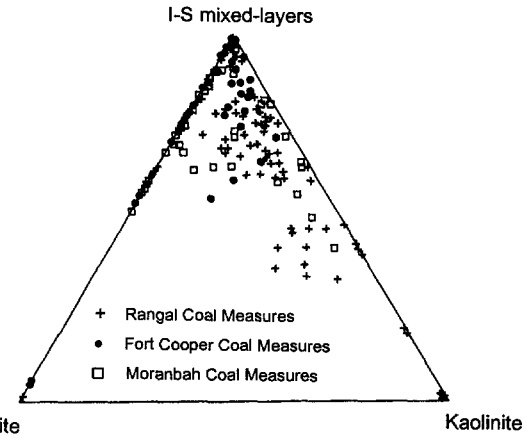

Figure 4. Relative amounts of three clay mineral components (I-S, chlorite, and kaolinite) in the <2-μm fraction from the northern Bowen Basin Coal Measures.

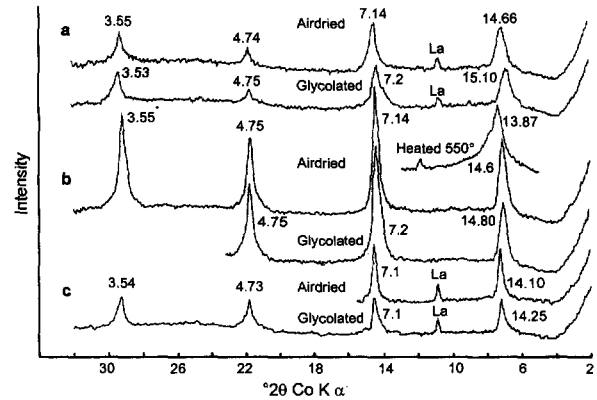

Figure 5. X-ray diffraction patterns of chlorite-rich C-S of <2-μm fractions from Cockatoo Creek 1 borehole. (a) Sample CK 1-6, tuff (Flat Top Formation, 2574 m). (b) Sample CK 1-12, volcanic rock (Barfield Formation, 3680 m). (c) Sample CK 1-13, volcanic rock (Barfield Formation, 3681 m). La = laumontite. Numbers above peaks are *d* values in Å.

Chlorite occurs preferentially in the 0.2–2-μm size fraction. Most of the chlorite shows very weak first- and third-order reflections at ~14.1–14.2 Å (001) and 4.74 Å (003), which is characteristic of Fe-rich chlorite (Moore and Reynolds, 1989). The Fe-rich chlorite was observed usually in samples where less illitic R = 0 and (R = 1) I-S and kaolinite predominate. In such samples, the distinction between chlorite and kaolinite was based on observing the 002 peak of kaolinite at 3.58 Å and 004 peak of chlorite at 3.53 Å (Figure 3c). Further, heating of the samples to 550°C for 1 h results in complete destruction of kaolinite and an increase of the 001 reflection of chlorite, and thus confirms the presence of chlorite.

Some chlorites in samples from the Fort Cooper and Moranbah Coal Measures show significant intensity of 001 and 003 peaks relative to even-order peaks (Figure 3d), which is indicative of a high Mg content in chlorites (Moore and Reynolds, 1989; Hillier *et al.*, 1996). These chlorites (Fe,Mg-rich chlorites) are associated with high proportions of illite in I-S and the lack of kaolinite.

Several clay separates from the Cockatoo Creek 1 borehole consist of chloritic minerals which contain small amounts of expandable layers (Figure 5). After ethylene-glycol solvation of the air-dried samples, the interstratified chlorite-smectite (C-S) 001/001 reflection increases to d = 14.3–15.1 Å (Figure 5a and 5b). Furthermore, this change in d value of the 001/001 peak, after heating for 1 h at 550°C (Figure 5a), confirms the presence of chlorite-smectite. These clays are defined (Moore and Reynolds, 1989) as randomly interstratified C-S with a smectite content of <10%.

Zeolites, such as analcime and laumontite, were identified in the samples from the Cockatoo Creek 1 borehole. Analcime is found in a shallow siltstone sample, whereas laumontite is detected in the pyroclastic and volcanic rocks from the deeper part of the borehole. In the northern Bowen Basin, zeolite is not evident in the Late Permian coal measures.

Sandstone petrography

Texture, morphology, and mineral paragenesis of the authigenic clay minerals are summarized in Table 1, and some representative examples are shown in Figures 6 to 10. SEM and TEM observations show that the I-S exhibits different morphologies depending on the ordering type (Figures 7 and 8). Smectite-rich, randomly interstratified I-S occurs as crenulated and irregular flakes (Figure 7A), a typical morphology for such clays (Welton, 1984; Keller *et al.*, 1986). By TEM, R = 0 and R = 1 type I-S samples from mudrocks are characterized as hexagonal-shaped particles with occasional rounded edges (Figure 8A). This latter effect is attributed to dissolution of unstable clay phases (Whitney and Velde, 1993). SEM observations of the short-range ordered (R = 1) I-S show slightly crenulated flakes indicative of irregular flattening of plates (Figure 6A), which is associated with a higher illite content (Keller *et al.*, 1986). In contrast, R ≥ 3 type illitic clays with >85% illite layers are composed of euhedral laths and plates (Figures 7B and 8B). The laths, set regularly at 60° and 120° to each other, coalesce to laminated platy crystals. Similar authigenic illite in the pore space of sandstones was described by Güven *et al.* (1980).

Clay mineral distribution

Northern Bowen Basin. Changes in clay-mineral compositions with depth and changes in composition with spatial correlations were studied in 35 boreholes. The clay-mineral evolution in six representative boreholes

https://doi.org/10.1346/CCMN.2000.0480306 Published online by Cambridge University Press

Table 1. Summary of texture, morphology, and assemblages of the authigenetic clay minerals.

Mineral	Texture	Morphology	Paragenesis
I-S	grain coating; replacement after feldspar, rock fragments, and mica; fracture and pore-fillings	R = 0 and (R = 1) I-S: flakes (R ≥ 3) I-S: laths	synchronous with kaolinite and chlorite; no kaolinite with (R ≥ 3) I-S; postdates Ca,Fe,Mg-rich carbonates
Chlorite	chamosite replacement after rock fragments and ferromagnesian minerals. Fe,Mg-rich chlorite: associated with dissolution of volcanic rock fragments; pore-lining rims and pore-fillings	sheet-like flakes; pseudo-hexagonal crystals	Fe,Mg-rich chlorite only with highly illitic (R ≥ 2) I-S
Kaolinite	replacement after feldspar and volcanic rock fragments; pore-filling	face to face stacks of pseudo-hexagonal plates; elongate "verms"	kaolinite only with R = 0 and (R = 1) I-S and chamosite; postdates dissolution of ankerite cements

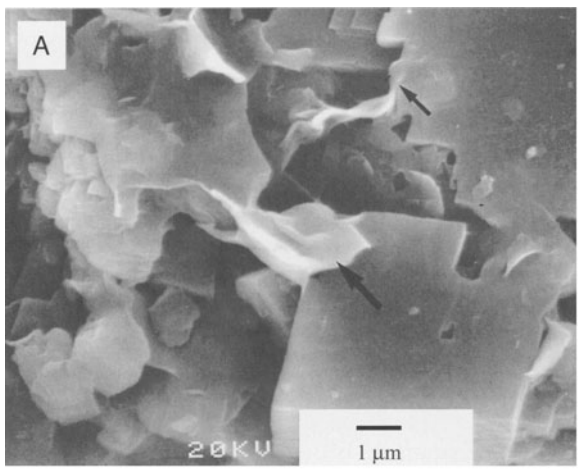

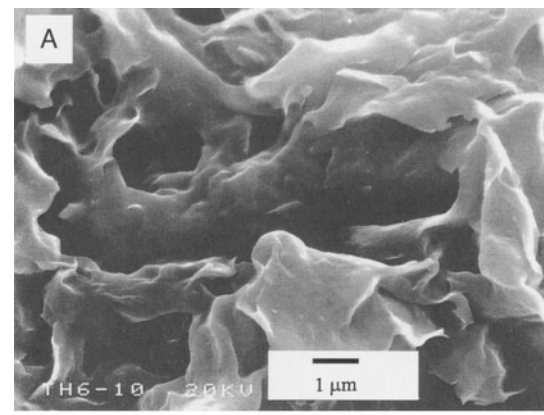

Figure 6. SEM and thin section photomicrographs illustrating textural features of I-S in sandstones. (A) I-S (R = 1) (arrow) coating ankerite crystals (sample DR 24-1, Moranbah Coal Measures, 120 m). (B) I-S pore linings (arrow) covering detrital grains (volcanic-rock fragments) (sample GR 12-10, Moranbah Coal Measures, 519.5 m, field of view = 0.7 mm wide).

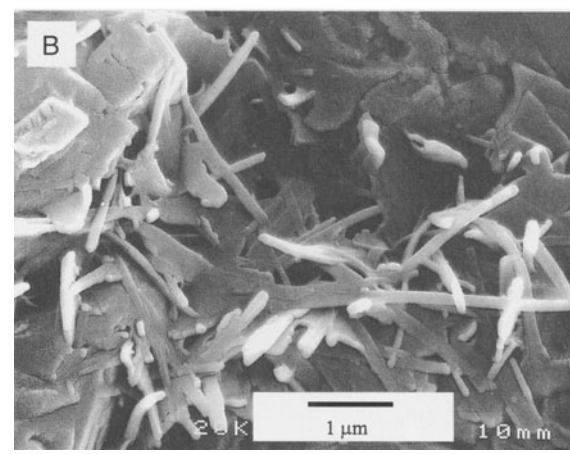

Figure 7. SEM photomicrographs illustrating morphological features of I-S in sandstones. (A) R = 0 type I-S containing ~65% expandable layers shows crenulated and irregular flakes (sample TH 6-10, Baralaba Coal Measures, 306.4 m). (B) R ≥ 3 type I-S containing <10% expandable layers shows lath-shaped crystals (sample C 510-10, Fort Cooper Coal Measures, 394.4 m).

https://doi.org/10.1346/CCMN.2000.0480306 Published online by Cambridge University Press

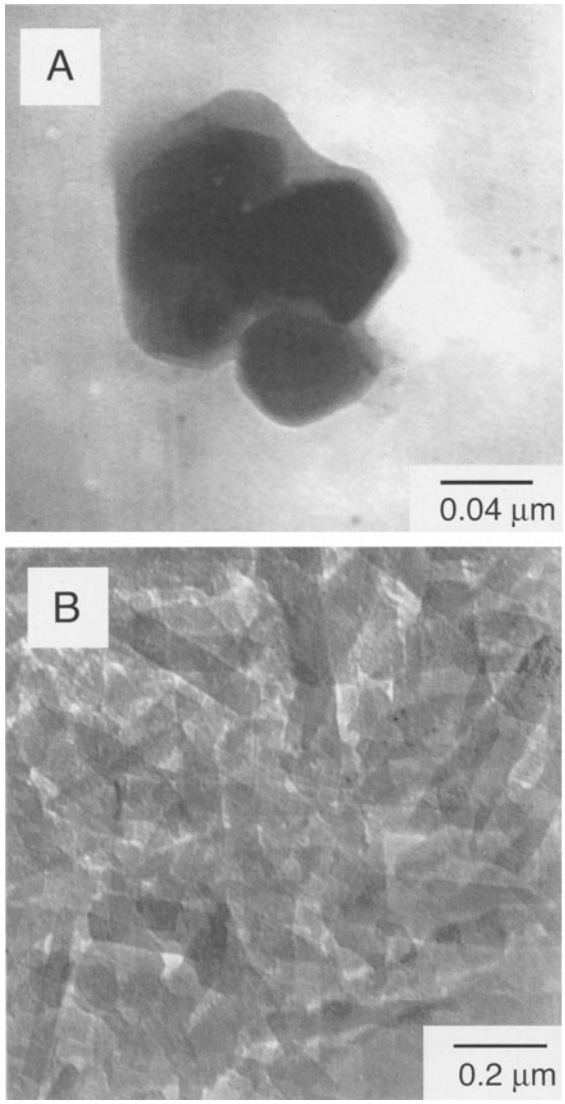

Figure 8. TEM photomicrographs illustrating morphological features of I-S. (A) Aggregate of smectite-rich (R = 0) I-S from a fine-grained sandstone-siltstone shows partly rounded, euhedral, hexagonal crystals (sample TH 6-10, Baralaba Coal Measures, 306.4 m). (B) Euhedral lath-like crystals of R ≥ 3 type I-S from a mudstone (sample WH 2-9, Fort Cooper Coal Measures, 320 m).

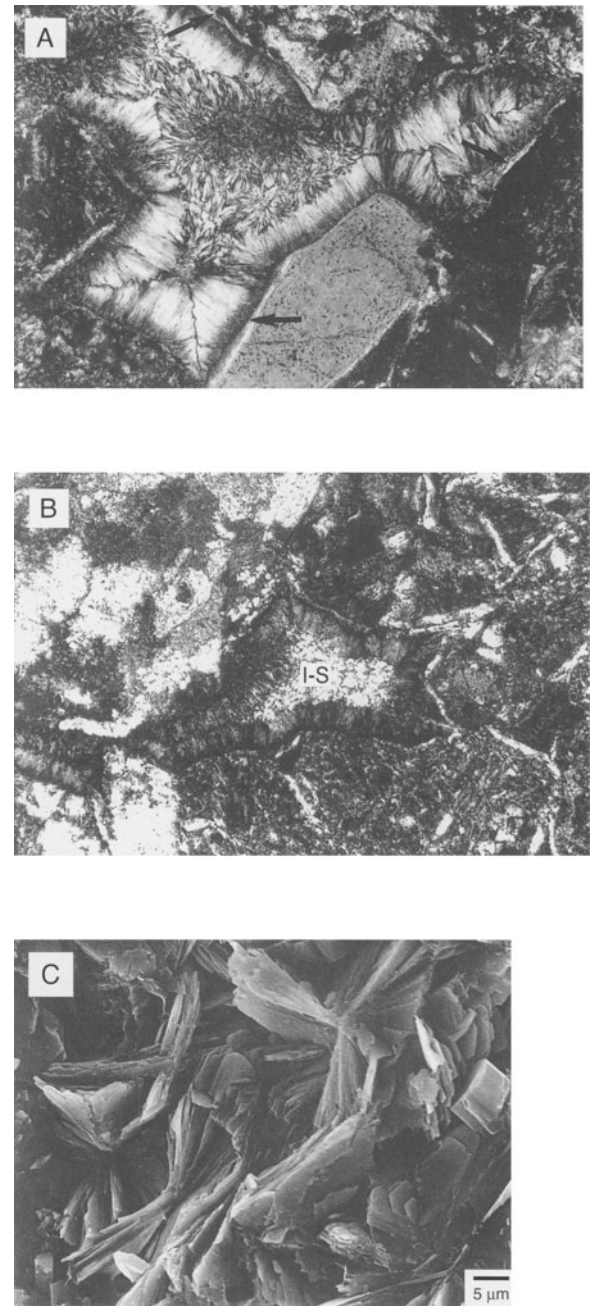

Figure 9. Thin section and SEM photomicrographs illustrating textural and morphological features of chlorite in sandstones. (A) Radial arrangement of chlorite flakes on detrital grains and filling of pore space by clusters of fan-shaped chlorite flakes. Note also the pore-lining illite between the chlorite and detrital grains (arrow) (sample DR 26-172, Moranbah Coal Measure, 172 m, field of view = 0.7 mm wide). (B) Center of a chlorite-rimmed pore space is filled by I-S cement (sample DR 26-2, Moranbah Coal Measures, 51.8 m, field of view = 0.7 mm wide). (C) SEM image of pore-filling chlorite showing subhedral to euhedral sheet-like crystals (sample GR 71-2, Fort Cooper Coal Measures, 39.6 m).

in the northern Bowen Basin is shown in Figures 11 to 15.

Borehole C 16 is situated on the western margin of the northern Bowen Basin (Figure 1), and contains Rangal Coal Measures and Fort Cooper Coal Measures (Figures 11 and 12). Boreholes WH 2 and GR 71 are separated by 15 km in the central part of the northern Bowen Basin (Figure 1). WH 2 includes Rangal and Fort Cooper Coal Measures, whereas in GR 71 the lower part of the Fort Cooper Coal Measures and the Moranbah Coal Measures are intersected (Figures 13 and 14). Borehole DR 26 is the northernmost borehole

https://doi.org/10.1346/CCMN.2000.0480306 Published online by Cambridge University Press

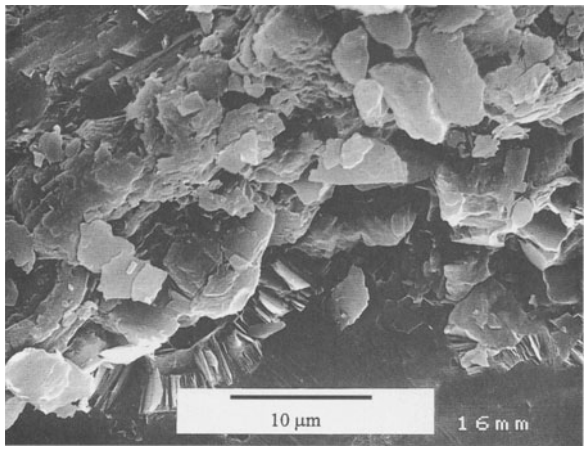

Figure 10. SEM photomicrograph illustrating a vermicular kaolinite enclosed within quartz cement in a sandstone (sample C 510-2, Rangal Coal Measures, 284 m).

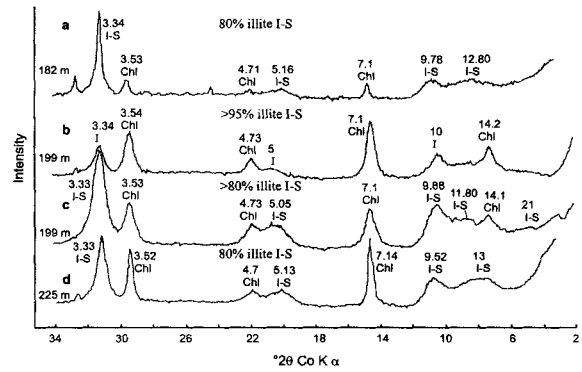

Figure 12. Representative X-ray diffraction patterns illustrating variations of clay mineral and I-S layer composition with depth in borehole C 16. (a) sample C 6-8, <2- µm fraction; (b) sample C 16-9, <2-µm fraction from sandstone; (c) sample C 16-9, <0.2-µm fraction from mudstone; (d) sample C 16-10, <2-µm fraction. All clay fractions are glycolated. I = illite, chl = chlorite. Numbers above peaks are *d* values in Å.

in the study area (Figure 1) and contains a representative section of the Moranbah Coal Measures (Figure 15).

The Rangal Coal Measures are characterized by a clay-mineral assemblage of (R = 1) I-S, kaolinite, and chlorite. Highly illitic I-S with an illite content of >80% and (R ≥ 3) I-S does not occur in samples from the Rangal Coal Measures. Kaolinite is common. Chlorite occurs in most of the samples, but it is not abundant.

In the Fort Cooper and Moranbah Coal Measures, I-S is generally more abundant (Figure 4). As observed in the Rangal Coal Measures, I-S does not show regular changes in illite content and Reichweite type with depth. The XRD patterns of the clay sepa-

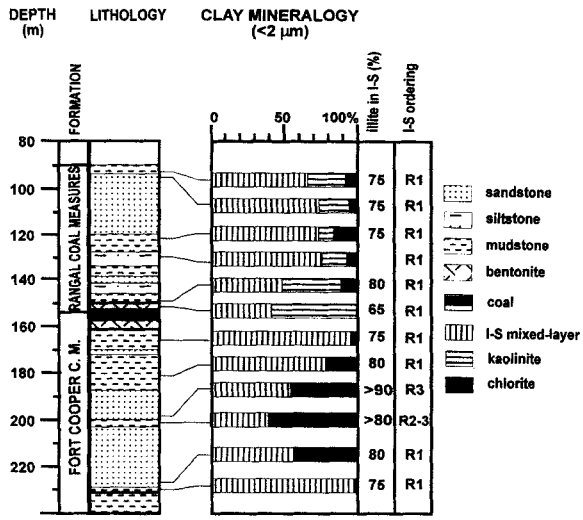

Figure 11. Distribution of clay minerals and variation of I-S layer composition and ordering type with depth in borehole Cairns County N.S. 16 (C 16).

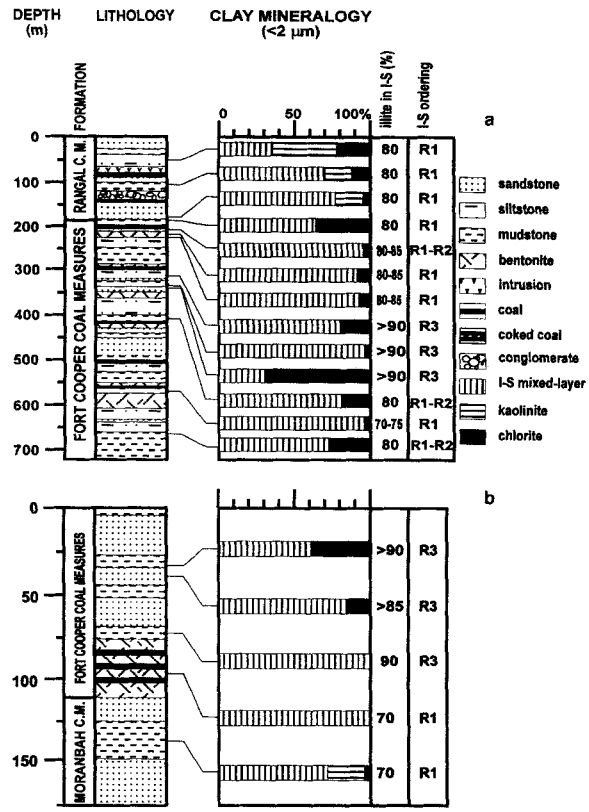

Figure 13. Distribution of clay minerals and variation of I-S layer composition and ordering type with depth in boreholes (a) Wodehouse N.S. 2 (WH 2) and (b) Grosvenor N.S. 71 (GR 71). Stratigraphic columns modified after Scott (1987).

https://doi.org/10.1346/CCMN.2000.0480306 Published online by Cambridge University Press

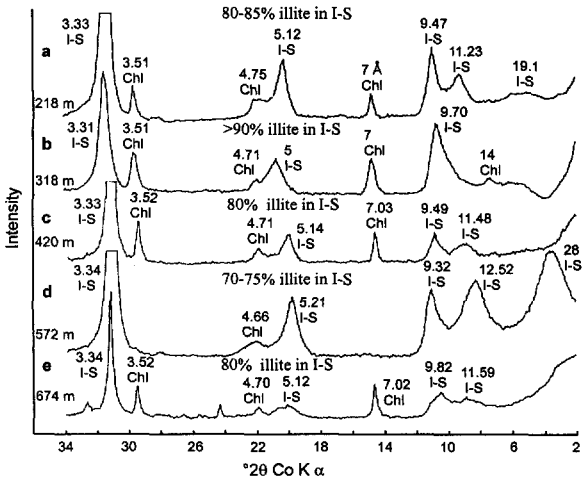

Figure 14. Representative X-ray diffraction patterns illustrating variations of clay mineral and I-S layer composition with depth in borehole WH 2. (a) sample WH 2-6, bentonite, <2-μm fraction; (b) sample WH 2-8, mudstone, <2-μm fraction; (c) sample WH 2-10, mudstone, <2-μm fraction; (d) sample WH 2-11, mudstone, <0.2-μm fraction; (e) sample WH 2-12, mudstone, <2-μm fraction. All clay fractions are glycolated. Chl = chlorite. Numbers above peaks are *d* values in Å.

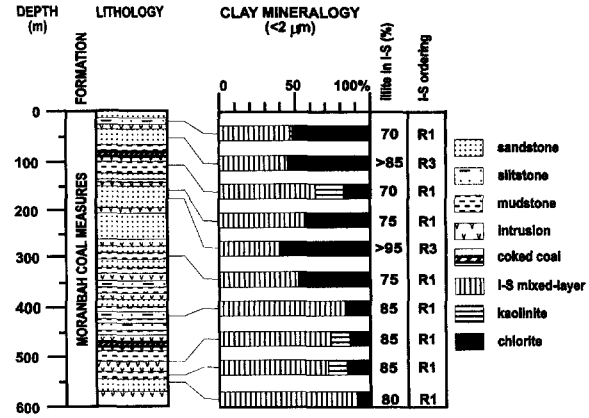

Figure 15. Distribution of clay minerals and variation of I-S layer composition and ordering type with depth in borehole Drake N.S. 26 (DR 26). Stratigraphic column modified after Scott (1987).

rations show an alternation of zones marked by various I-S Reichweite types and associated clay-mineral phases. Chlorite is ubiquitous and, as noted above, Fe,Mg-rich chlorite may become abundant in association with illite-rich I-S. This assemblage is characteristic of the clay-mineral distribution in the Fort Cooper and Moranbah Coal Measures. In contrast to the Rangal Coal Measures, kaolinite is not common, and occurs only occasionally in high abundance in the Moranbah Coal Measures. In summary, there is no systematic change in clay-mineral compositions with depth and spatially in the Late Permian coal measures of the northern Bowen Basin. Changes in clay-mineral distributions, and compositional and structural variations in the I-S phases are irregular and erratic.

Southern Bowen Basin. The Baralaba Coal Measures, which are equivalent to the Rangal Coal Measures of the northern Bowen Basin, were sampled in four boreholes in the Theodore area (Figure 1). The clay fraction of sandstones and mudrocks consists dominantly of I-S which shows only R = 0 ordering with <10 to ~50% illite. Kaolinite is present in all samples, but is not as abundant as in the northern part of the Bowen Basin. Many samples also contain chlorite in smaller amounts.

The Cockatoo Creek 1 borehole, ~60 km south of the Theodore area (Figure 1), was sampled at depths ranging from 1127 to 3681 m. The (R = 0) I-S is present only at the top of the borehole, and (R = 1) I-S occurs at 1254 m. The lack of kaolinite and the presence of (R ≥ 3) I-S are observed at 1700 m. Sandstone and mudstone samples in the lower part are characterized by clay assemblages of highly illitic (R ≥ 3) I-S and Fe-rich chlorite. Clay separations from one pyroclastic rock at 2574 m and two volcanic lavas at 3680–3681 m consist of chlorite-rich C-S and laumontite (Figure 5). The latter is also found as a vein mineral.

DISCUSSION

Clay-mineral distribution

In contrast to the depth-dependent evolution of clay minerals observed in deeply buried diagenetic environments (Hower *et al.*, 1976; Jennings and Tompson, 1986), the most striking characteristic of the Bowen Basin clays is the apparent erratic changes in mineralogy within brief stratigraphic intervals. Because temperature regularly increases with depth in these boreholes on the basis of vitrinite reflectance profiles (Beeston, 1981), the distribution of clay minerals is not related to temperature variations. Such distributions may be related to lithologic variations owing to differences in detrital sources or to randomly distributed detrital clay minerals (*e.g.,* Shaw and Primmer, 1991; Pollastro, 1993; Deng *et al.*, 1996). Petrology of the sandstone, however, indicates a single volcanic origin of the detrital components. Although iron and magnesium content in chlorite seems to be influenced by local lithological variations (see below), there is no evidence of direct control of lithology on illitization. The presence of some potassium-bearing detrital minerals in all rocks containing less illitic I-S suggests that insufficient potassium does not result in an apparent irregular distribution of I-S. Except for some mica minerals, which occur as relatively coarse grains, samples contain no other detrital phyllosilicate minerals. Petrographic evidence showing the authigenic char-

https://doi.org/10.1346/CCMN.2000.0480306 Published online by Cambridge University Press

acter of the clays (Figures 6 to 10) and the consistent K-Ar ages of ~210 Ma for I-S (Uysal *et al.,* 2000b) excludes a possibility of detrital influence. Thus, the effect of a detrital component on the clay-mineral distributions can be ruled out. Clay-mineral reactions in the northern Bowen Basin also can not be related to the effect of thin igneous intrusions, because the intrusions are much younger, Cretaceous age, and the effect of the intrusions on clay mineral reactions is limited to narrow zones immediately adjacent to intrusive bodies (Uysal, 1999).

Similar vertical variability and zonation of clay minerals were observed by Whitney and Northrop (1987) and Owen *et al.* (1989) in the San Juan Basin, and are explained by changes in flow rates and chemistry of migrating fluids. Such distributions of clay minerals in hydrothermal environments is common, and results from variability in the pore-fluid composition controlled largely by variable fluid/rock ratios as a result of variations in permeability (*e.g.,* 1977; Harvey and Browne, 1991; WoldeGabriel and Goff, 1992).

Illite-smectite

Morphological significance of I-S. Textural data from the sandstones suggest the authigenic character of the I-S; flakes of I-S occur on euhedral (authigenic) carbonate minerals and well-defined lath-shaped I-S crystals are present also (Figures 6 to 8). Similar habits of neoformed illite in sandstones were documented by others (*e.g.,* Güven *et al.,* 1980; McHardy *et al.,* 1982; Nadeau *et al.,* 1985; Huang, 1992). I-S particles in mudrocks also have euhedral shapes and thus are interpreted to be authigenic also (Figure 8).

The variable morphology of authigenic illite was attributed to variations in porosity and permeability of the host rock (Glasmann *et al.,* 1989; Inoue *et al.,* 1990). Lath-shaped illite occurs commonly in environments of high porosity and permeability, which enable free fluid circulation and unrestrained crystal growth. This morphology is commonly observed in sandstones, where a dissolution and a neoformation process is widely accepted (Jeans, 1989). In contrast, illitic clays from rocks having low porosity and permeability, such as mudstones and bentonites, form commonly by replacement of the smectite precursor and inherit the texture (Ahn and Peacor, 1986; Inoue *et al.,* 1990). Thus, in deeply buried pelitic rocks or bentonites, no morphological changes occur during illitization, which is characteristic for the solid-state transformation mechanism (Inoue *et al.,* 1990). However, euhedral, lath-shaped morphology of the illitic clays can also develop by neoformation from solution in fine-grained argillaceous rocks and bentonites at relatively high water/rock ratios, such as hydrothermal environments (Yau *et al.,* 1987, 1988; Christidis, 1995), or sedimentary basins, where relatively high porosity and water/rock ratios occur when the sediment is not greatly compacted during deep burial (Glasmann *et al.,* 1989).

In the present study, the morphological variations of the illitic clays correlate with changes in the Reichweite type, which may indicate changes in porosity, permeability, and reaction mechanism. The smectite-rich R = 0 and less illitic (R = 1) I-S are characterized only by flakes, and illite-rich clays (R $\geq$ 3) display laths, in accordance with Keller *et al.* (1986). In contrast, Inoue *et al.* (1987) and Christidis (1995) showed that lath-shaped crystals first appear at 80% expandability, and increase gradually in amount with decreasing expandable layers, resulting from the dissolution of the smectite component. In the current study, however, no lath-shaped crystals coexist with less illitic flakes. The various morphologies of I-S coincide with R = 0 and R = 1 ordering (flakes) to R $\geq$ 3 ordering (laths; see Figures 7 and 8). These results suggest the direct precipitation of the highly illitic I-S from circulating fluids interacting with early-formed smectite, smectite-rich I-S, and/or glassy volcanic rock fragments, rather than a consecutive smectite-to-illite conversion process as described by Inoue *et al.* (1992).

Fluid chemistry may be another factor influencing the illitic-clay precipitation and the growth texture. Huang (1992) showed that illite laths are favored by neutral hydrothermal solutions, whereas the flakes formed mostly under acidic or alkaline conditions.

Effect of porosity-permeability on I-S distribution. The occurrence of lath-shaped I-S associated with R $\geq$ 3 ordering in sandstones and adjacent mudstones requires transport of potassium-bearing fluids at relatively high water/rock ratios. This condition requires high porosity and permeability to promote circulation of neutral solutions with a relatively high $\alpha_{K^+}/\alpha_{H^+}$ ratio where α = activity. In contrast, the formation of smectite-rich (R = 0) I-S and (R = 1) I-S with flake-like morphology seems to result from lower fluid activity owing to a lower water/rock ratio and consequently a limited supply of potassium. This observation may suggest that water/rock ratio and potassium availability may have controlled the illitization reaction. Changes in permeability may determine the variable water/rock ratio and potassium availability and consequently, degree of illitization to produce different Reichweite values. Similarly, the effect of permeability on variable illite content in I-S has been recognized in different hydrothermal environments (*e.g.,* Reyes, 1990; Flexser, 1991; WoldeGabriel and Goff, 1992; Šamajová *et al.,* 1993; Patrier *et al.,* 1996). In our study, the degree of illitization, and consequently the permeability is generally not controlled by primary rock lithology. For instance, many medium to coarse-grained sandstone samples contain less illitic I-S, whereas many clay samples of highly illitic (R $\geq$ 3) I-S are from the interior of relatively thick mudstones.

Such occurrences are probably related to fracture-enhanced permeability and fluid circulation. Crosscutting fractures and faults resulting from the Hunter-Bowen Orogeny are abundant in the Bowen Basin Coal Measures and extensively mineralized with carbonates and clays (Pattison *et al.,* 1996; Golding *et al.,* 1999; Uysal, 1999). Relatively high water/rock ratios are expected to prevail in such fracture-enhanced permeable zones. The irregular distribution of (R ≥ 3) I-S is associated with significant ^{18}O depletion in the oxygen-isotope composition of these clays, which is interpreted as a result of high water/rock ratios related to fluid flow (Uysal, 1999). The abundance of water in such fracture-enhanced environments can affect the extent of illitization significantly, as shown experimentally by Whitney (1990).

These conclusions are consistent with a hydrothermal origin for the northern Bowen Basin clays. On the basis of K-Ar and Rb-Sr ages of the illitic clays, the hydrothermal systems are attributed to a Late Triassic extensional tectonic event in eastern Queensland which most significantly affected the northern part of the basin (Uysal *et al.,* 2000b). This event is also responsible for an overall increase in geothermal gradient in the entire Bowen Basin.

Source of potassium. One important model for illite formation involves potassium release into fluids by dissolution of K-bearing silicate minerals. These solutions may originate from deeper parts of the basin to the sites of illitization in a chemically open system (Chaudhuri and Clauer, 1993; Awwiller, 1993; Furlan *et al.,* 1996; Lynch, 1997). Feldspars, micas, and volcanic-rock fragments (especially the felsic rocks) occurring in the sandstone, are possible sources for the potassium and aluminum. The presence of relatively fresh K-rich feldspars and mica in some highly illitic samples suggests that the potassium consumed for illitization originated primarily from outside. To a lesser extent, local supply of potassium is also possible. Dissolution of K-bearing phases by organic acids generated during hydrocarbon maturation (Eberl, 1993; Small, 1994) may enhance illitization in organic-rich rocks (O'Shea and Frape, 1988; Li *et al.,* 1997), and may account for higher proportions of illite in I-S in some organic-rich mudstones in the Basin.

Chlorite

Chamosite and Fe,Mg-rich chlorite exhibit different textural characteristics and mineral associations in the Basin. These differences may reflect two origins of the chlorite.

Chamosite occurs throughout the stratigraphic section, but generally in low amounts. They are associated mostly with less illitic I-S of R = 0 and R = 1 ordering and kaolinite, and less commonly with (R ≥ 3) I-S. Chamosite usually occurs as direct replacements of glassy volcanic-lithic grains or the earlier-formed alteration products such as smectite and ferromagnesian silicate minerals. A similar occurrence of chlorite is known from the Wairakei geothermal area, New Zealand, where chlorite forms from *in situ* hydrothermal alteration and replacement of volcanic glass (Steiner, 1977).

Changes in chlorite composition are correlated with chlorite abundance and texture. Chlorite showing a relatively high Mg content is more abundant and associated with highly illitic clays. These Fe,Mg-rich chlorites occur as clay rims and pore-filling cements, and develop as euhedral to subhedral crystals. They occur in narrow zones in the deeper parts of the coal measures.

The Fe,Mg-rich chlorite does not show any inherited morphology, and thus it seems unlikely that this chlorite originated by transformation from a precursor smectite through an interstratified chlorite-smectite (*e.g.,* Dunoyer de Segonzag, 1970; Curtis *et al.,* 1985; Hillier, 1994). Formation of the chlorite from kaolinite (*e.g.,* Boles and Franks, 1979) is not consistent with our petrographic observations. Our observations show no evidence of such a reaction. A reaction between illitic clays and Fe,Mg-rich carbonates (Hutcheon *et al.,* 1980; Hillier, 1993) also does not explain the origin of the chlorite, because in samples containing abundant chlorite, ankerite is present generally as well-shaped euhedral crystals and any dissolution reaction would have corroded these crystals. The precipitation of chlorite is associated with dissolution of the volcanic lithic fragments. Textural relationships suggest that the precipitation of highly illitic I-S proceeded in several steps separated by periods of dissolution of lithic fragments and crystallization of chlorite. Therefore, we conclude that high flow rates of illite-forming fluids in highly permeable zones in the Bowen Basin Coal Measures may have induced the dissolution of labile volcanic-rock fragments, thereby resulting in enrichment of fluids for Al, Fe, and Mg required for chlorite formation. Although Fe,Mg-rich chlorite is always associated with highly illitized (R ≥ 2) I-S, the latter may occur also with chamosite. Local variations in availability of iron and magnesium may be related to parent-rock compositions. For example, sandstones with more intermediate-and mafic-rock fragments are rich in iron and magnesium, which facilitate the formation of Fe,Mg-rich chlorite. Similarly, the occurrence of chlorite-rich C-S minerals in the Cockatoo Creek 1 borehole in the southern Bowen Basin seems to be lithology related. These Mg-rich chlorites are observed only in basic-intermediate pyroclastic and volcanic rocks and in one volcaniclastic-sandstone sample, although other sandstones from the borehole are also volcanic in origin. Restriction of the occurrence of C-S to certain rock types suggests that the original rock composition is an important factor

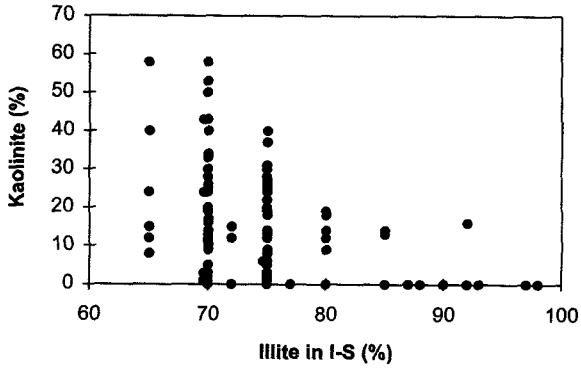

Figure 16. Percent kaolinite in the clay fractions *vs.* the proportion of illite in I-S.

controlling the type of chloritic minerals. Pyroclastic or volcanic rocks with abundant mafic components, or sandstones with mafic lithic fragments favor the formation of a C-S phase because these rocks are important sources for magnesium.

Kaolinite

Petrographic observations of sandstones reveal that kaolinite forms by dissolution of volcanic-rock fragments, micas, and alteration of feldspars. Two main processes, thermal maturation of organic matter and meteoric water-flow, supply dilute and acidic solutions possibly responsible for grain dissolution and kaolinite precipitation (Surdam *et al.,* 1989; Bjørlykke, 1998).

Grain leaching and kaolinite formation in the Late Permian coal measures may be related to numerous coal seams and organic-rich mudrocks that are a potential source of CO_2. In some instances, kaolinite was observed to occur preferentially in the adjacent rocks of coal seams or in rocks rich in organic matter. However, rocks closely associated with organic-rich mudrocks and coal seams may contain no kaolinite. These observations imply that the contribution of acidic solutions, derived from organic-rich rocks, to grain dissolution and precipitation of authigenic kaolinite is limited and only locally important. Baker and Golding (1992) concluded that the authigenic kaolinite formed from meteoric water mobilized from the Late Triassic uplift of the Denison Trough sequence on the southwestern margin of the Bowen Basin. Stable-isotope data from samples of the northern part of the Basin (Uysal, 1999) confirm the meteoric origin of the fluids producing kaolinite. Stable-isotope compositions of illitic clays indicate that solutions involved in illite formation were also meteoric in origin. Radiometric dating of the illitic clays suggests a Late Triassic timing for illite formation (Uysal *et al,* 2000b), which is contemporaneous with hydrothermal processes from a Late Triassic regional extension in eastern Australia. In contrast to Baker and Caritat (1992), who related illitization to mesogenetic burial diagenesis during Middle to Late Triassic time, the results presented here imply that kaolinite and illitic clays are coeval and their formation was controlled by the same paleohydrologic event.

Kaolinite is ubiquitous in the Rangal Coal Measures (Figure 4). Generally, it is subordinate in abundance to I-S, but samples (especially mudrocks) may contain kaolinite as the main or the only authigenic clay phase, sometimes with trace amounts of I-S. Less commonly, kaolinite is abundant in samples from the deeper parts of the coal measures, where it is irregularly distributed and confined to samples where I-S is relatively less illitic. XRD data show an inverse relationship between kaolinite abundance and the proportion of illite in I-S for clay samples from the northern part of the Bowen Basin (Figure 16). Highly illitic ($R \geq 3$) I-S rocks do not contain kaolinite (except for one sample subjected to contact metamorphism), and where kaolinite is abundant, clays are less illitic (Figure 16). The occurrence of I-S and kaolinite is best explained by the assumed ratios of activities of K^+ and H^+ of the fluids. In the Fort Cooper and Moranbah Coal Measures, highly illitized zones without kaolinite may have been produced by potassium-rich solutions from deeper parts of the basin. Away from these zones, for instance in the shallow sections in the Rangal Coal Measures and in horizons of low permeability, the $\alpha_{K^+}/\alpha_{H^+}$ of the fluids is probably sufficiently low that the precipitation of kaolinite is favored. Potassium availability and/or acidic fluid supply will determine the relative amount of kaolinite coexisting with less illitic I-S. Fluids with initially low pH will induce the dissolution of micas and volcanic-rock fragments and concomitant precipitation of kaolinite. Potassium released during this process cannot be removed because at low-permeability conditions, very slow, diffuse fluid flow is expected to occur. As a result, the $\alpha_{K^+}/\alpha_{H^+}$ ratio of the fluid will increase and kaolinite will no longer be stable, and consequently I-S formation will be favored.

Zeolites

Zeolites are absent in the volcaniclastic rocks in the northern part of the Bowen Basin, where ubiquitous and often abundant carbonate minerals suggest relatively high $\alpha_{CO_2}/\alpha_{H_2O}$ ratios; however, analcime and laumontite are found from the Cockatoo Creek 1 borehole in the southern Bowen Basin. The formation of zeolites is strongly controlled by the rock type or composition of the detrital components, with little or no cations derived from outside the system (Surdam and Boles, 1979; Vavra, 1989). In the Cockatoo Creek 1 borehole, for example, newly formed laumontite is restricted to intermediate or mafic pyroclastic rocks and volcanic lavas.

ACKNOWLEDGMENTS

The authors thank K. Kyser, M. Coleman, T. Frank, and M. Glikson for constructive comments on an earlier version

of this paper. Critical reviews and useful comments by E. Daniels and an anonymous reviewer are greatly appreciated, as is editorial handling by S. Guggenheim and S. Altaner. Financial support for this project from the Queensland Transmission and Supply Corporation and Energy Research and Development Corporation is gratefully acknowledged. Thanks also to the Queensland Mines Department, The Shell Company Australia, Newslands, German Creek, and Yarrabee Coal Companies for access to drill-core material.

REFERENCES

Ahn, J.H. and Peacor, D.R. (1986) Transmission and analytical electron microscopy of the smectite-illite transition. *Clays and Clay Minerals,* **34,** 165–179.

Awwiller, D.N. (1993) Illite/smectite formation and potassium mass transfer during burial diagenesis of mudrocks: A study from the Texas Gulf Coast Paleocene-Eocene. *Journal of Sedimentary Petrology,* **63,** 501–512.

Baker, J.C. and Caritat, P. de (1992) Postdepositional history of the Permian Sequence in the Denison Trough, eastern Australia. *American Association of Petroleum Geologists Bulletin,* **76,** 1224–1249.

Baker, J.C. and Golding, S.D. (1992) Occurrence and palaeohydrological significance of authigenic kaolinite in the Aldebaran Sandstone, Denison Trough, Queensland, Australia. *Clays and Clay Minerals,* **40,** 273–279.

Baker, J.C., Fielding, C.R., Caritat, P. de, and Wilkinson, M.M. (1993) Permian evolution of sandstone composition in a complex back-arc extensional to foreland basin: The Bowen Basin, Eastern Australia. *Journal of Sedimentary Petrology,* **63,** 881–893.

Beeston, J.W. (1981) Coal rank variation in the Bowen Basin. *Geological Survey of Queensland Record, Record 198/48.*

Biscaye, P.E. (1965) Mineralogy and sedimentation of recent deep-sea clay in the Atlantic Ocean and adjacent seas and oceans. *Geological Society of America Bulletin,* **76,** 803–832.

Bjørlykke, K. (1998) Clay mineral diagenesis in sedimentary basins—a key to the prediction of rock properties. Examples from the North Sea Basin. *Clay Minerals,* **33,** 15–34.

Boles, J.R. and Franks, S.G. (1979) Clay diagenesis in Wilcox sandstones of southwest Texas: Implications of smectite diagenesis on sandstone cementation. *Journal of Sedimentary Petrology,* **49,** 55–70.

Bühmann, C. (1992) Smectite-to-illite conversion in a geothermally and lithologically complex Permian sedimentary sequence. *Clays and Clay Minerals,* **40,** 53–64.

Chaudhuri, S. and Clauer, N. (1993) Strontium isotopic compositions and potassium and rubidium contents of formation waters in sedimentary basins: Clues to the origin of the solutes. *Geochimica et Cosmochimica Acta,* **57,** 429–437.

Christidis, G.E. (1995) Mechanism of illitization of bentonites in the geothermal field of Milos Island Greece: Evidence based on mineralogy, chemistry, particle thickness and morphology. *Clays and Clay Minerals,* **43,** 569–585.

Curtis, C.D., Hughes, C.R., Whiteman, J.A., and Whittle, C.K. (1985) Compositional variation with some sedimentary chlorites and some comments on their origin. *Mineralogical Magazine,* **49,** 375–386.

Deng, X., Sun, Y., Lei, X., and Lu, Q. (1996) Illite/smectite diagenesis in the NanXiang, Yitong, and North China Permian-Carboniferous basins: Application to petroleum exploration in China. *American Association of Petroleum Geologists Bulletin,* **80,** 157–173.

Draper, J.J., Palmieri, V., Price, P.L., Briggs, D.J.C., and Parfrey, S.M. (1990) A biostratigraphic framework for the Bowen Basin. In *Bowen Basin Symposium 1990 Proceedings,* J.W. Beeston, ed., Geological Society of Australia, Sydney, 26–35.

Dunoyer de Segonzag, G. (1970) The transformation of clay minerals during diagenesis and low-grade metamorphism: A review. *Sedimentology,* **15,** 281–346.

Eberl, D.D. (1993) Three zones for illite formation during burial diagenesis and metamorphism. *Clays and Clay Minerals,* **41,** 26–37.

Esposito, K.J. and Whitney, G. (1995) *Thermal Effects of Thin Igneous Intrusions on Diagenetic Reactions in a Tertiary Basin of Southwestern Washington.* U.S. Geological Survey Bulletin 2085-C, Washington, D.C., 36 pp.

Fielding, C.R., Stephens, C.J., and Holcombe, R.J. (1997) Permian stratigraphy and palaeogeography of the eastern Bowen Basin, Gogango Overfolded Zone and Strathmuir Synclinorium in the Rockhampton-Mackay region, central Queensland. In *Tectonics and Metallogenesis of the New England Orogen,* P.M. Ashley and P.G. Flood, eds., Geological Society Australia Special Publication 19, Sydney, 80–95.

Flexser, S. (1991) Hydrothermal alteration and past and present thermal regimes in the western moat of Long Valley caldera. *Journal of Volcanology and Geothermal Research,* **48,** 303–318.

Furlan, S., Clauer, N., Chaudhuri, S., and Sommer, F. (1996) K transfer during burial diagenesis in the Mahakam Delta Basin (Kalimantan, Indonesia). *Clays and Clay Minerals,* **44,** 157–169.

Glasmann, J.R., Larter, S., Briedis, N.A., and Lundegart, P.D. (1989) Shale diagenesis in the Bergen High area, North Sea. *Clays and Clay Minerals,* **37,** 97–112.

Golding, S.D., Collerson, K.D., Uysal, I.T., Glikson, M., Baublys, K., and Zhao, J.X. (1999) Nature and source of carbonate mineralisation in coals of the Bowen Basin, eastern Australia: Implications for the origin of coal seam methane and other hydrocarbons sourced from coal. In *Organic Matter and Mineralisation: Thermal Alteration, Hydrocarbon Generation and Role in Metallogenesis,* M. Glikson and M. Mastalerz, eds., Kluwer Academic Press, Dordrecht, The Netherlands, 296–313.

Güven, N., Hower, W.F., and Davies, D.K. (1980) Nature of authigenic illites in sandstone reservoirs. *Journal of Sedimentary Petrology,* **50,** 761–766.

Harvey, C.C. and Browne, P.R. (1991) Mixed-layer clay geothermometry in the Wairakei geothermal field, New Zealand. *Clays and Clay Minerals,* **39,** 614–621.

Hillier, S. (1993) Origin, diagenesis, and mineralogy of chlorite minerals in Devonian lacustrine mudrocks, Orcadian Basin, Scotland. *Clays and Clay Minerals,* **41,** 240–259.

Hillier, S. (1994) Pore-lining chlorites in siliciclastic reservoir sandstones: Electron microprobe, SEM and XRD data, and implications for their origin. *Clay Minerals,* **29,** 665–679.

Hillier, S., Fallick, A.E., and Matter, A. (1996) Origin of pore-lining chlorite in the aeolian of Rotliegend of northern Germany. *Clay Minerals,* **31,** 153–171.

Hoffman, J. and Hower, J. (1979) Clay mineral assemblages as low grade metamorphic geothermometers: Application to the thrust faulted disturbed belt of Montana. In *Aspects of Diagenesis,* P.A. Scholle and P.S. Schluger, eds., Society of Economic Paleontologists and Mineralogists Special Publication 26, Tulsa, Oklahoma, 55–79.

Horton, D.G. (1985) Mixed-layer illite-smectite as a paleotemperature indicator in the Amethyst vein system, Creede district, Colorado, USA. *Contributions to Mineralogy and Petrology,* **91,** 171–179.

Hower, J., Eslinger, E.V., Hower, M.E., and Perry, E.A. (1976) Mechanism of metamorphism of argillaceous sediment: Mineralogical and chemical evidence. *Geological Society of America Bulletin,* **87,** 725–737.

Huang, W.L. (1992) Illitic-clay formation during experimental diagenesis of arkoses. In *Origin, Diagenesis and Petrophysics of Clay Minerals in Sandstones,* D.W. Houseknect, ed., Society of Economic Paleontologists and Mineralogists Special Publication 47, Tulsa, Oklahoma, 49–63.

Hutcheon, I., Oldershaw, A., and Ghent, E.D. (1980) Diagenesis of Cretaceous sandstones of the Kootenay Formation at Elk Valley (southeast British Columbia) and Mt. Allan (southwestern Alberta). *Geochimica et Cosmochimica Acta,* **44,** 1425–1435.

Inoue, A., Kohyama, N., Kitagawa, R., and Watanabe, T. (1987) Chemical and morphological evidence for the conversion of smectite to illite. *Clays and Clay Minerals,* **35,** 111–120.

Inoue, A., Watanabe, T., Kohyama, N., and Brusewitz, A.M. (1990) Characterization of illitization of smectite in bentonite beds at Kinnekulle, Sweden. *Clays and Clay Minerals,* **38,** 241–249.

Inoue, A., Utada, M., and Wakita, K. (1992) Smectite-to-illite conversion in natural hydrothermal systems. *Applied Clay Science,* **7,** 131–145.

Jeans, C.V. (1989) Clay diagenesis in sandstones and shales: An introduction. *Clay Minerals,* **24,** 127–136.

Jennings, S. and Thompson, G.R. (1986) Diagenesis of Plio-Pleistocene sediments of the Colorado River delta, southern California. *Journal of Sedimentary Petrology,* **56,** 89–98.

Keller, W.D., Reynolds, R.C., and Inoue, A. (1986) Morphology of clay minerals in the smectite-to-illite conversion series by scanning electron microscopy. *Clays and Clay Minerals,* **34,** 187–197.

Li, G., Peacor, D.R., and Coombs, D.S. (1997) Transformation of smectite to illite in bentonite and associated sediments from Kaka Point, New Zealand: Contrast in rate and mechanism. *Clays and Clay Minerals,* **45,** 54–67.

Lynch, F.L. (1997) Frio shale mineralogy and the stoichiometry of the smectite-to-illite reaction: The most important reaction in clastic sedimentary diagenesis. *Clays and Clay Minerals,* **45,** 618–631.

Mallett, C.W., Pattison, C., McLennan, T., Balfe, P., and Sullivan, D. (1995) Bowen Basin. In *Geology of Australian Coal Basins,* C.R. Ward, H.J. Harrington, C.W. Mallett, and J.W. Beeston, eds., Geological Society of Australia Special Publication 1, Sydney, 299–339.

McHardy, W.J., Wilson, M.J., and Tait, J.M. (1982) Electron microscope and X-ray diffraction studies of filamentous illitic clay from sandstones of the Magnus field. *Clay Minerals,* **17,** 23–39.

Moore, D.M. and Reynolds, R.C. (1989) *X-ray Diffraction and the Identification and Analysis of Clay Minerals.* Oxford University Press, Oxford, 322 pp.

Nadeau, P.H. and Reynolds, R.C. (1981) Burial and contact metamorphism in the Mancos shale. *Clays and Clay Minerals,* **29,** 249–259.

Nadeau, P.H., Wilson, M.J, McHardy, W.J., and Tait, J.M (1985) The conversion of smectite to illite during diagenesis: Evidence from some illitic clays from bentonites and sandstones. *Mineralogical Magazine,* **49,** 393–400.

O'Shea, K.J. and Frape, S.K. (1988) Authigenic illite in the Lower Silurian Cataract Group sandstones of southern Ontario. *Bulletin of Canadian Petroleum Geology,* **36,** 158–167.

Owen, D.E., Turner-Peterson, C.E., and Fishman, N.S. (1989) *X-ray Diffraction Studies of the <0.5-μm Fraction from the Brushy Basin Member of the Upper Jurassic Morrison Formation, Colorado Plateau.* U.S. Geological Survey Bulletin 1808-G, Washington, D.C., 25 pp.

Patrier, P., Papapanagiotou, P., Beaufort, D., Traineau, H., Bril, H., and Rojas, J. (1996) Role of permeability versus temperature in the distribution of the fine (<0.2 μm) clay fraction in the Chipilapa geothermal system (El Salvador, Central America). *Journal of Volcanology and Geothermal Research,* **72,** 101–120.

Pattison, C.I., Fielding, C.R., McWatters, R.H., and Hamilton, L.H. (1996) Nature and origin of fractures in Permian coals from the Bowen Basin, Queensland, Australia. In *Coalbed Methane and Coal Geology,* R. Gayer and I. Harris, eds., Geological Society Special Publication 109, London, 133–150.

Pollastro, R.M. (1990) The illite/smectite geothermometer—Concepts, methodology, and application to basin history and hydrocarbon generation. In *Applications of Thermal Maturity Studies to Energy Exploration,* V.F. Nuccio and C.E Barker, eds., Society of Economic Paleontologists and Mineralogists, Rocky Mountain Section, 1–18.

Pollastro, R.M. (1993) Considerations and applications of the illite/smectite geothermometer in hydrocarbon-bearing rocks of Miocene to Mississippian age. *Clays and Clay Minerals,* **41,** 119–133.

Ramseyer, K. and Boles, J.R. (1986) Mixed-layer illite/smectite minerals in Tertiary sandstones and shales, San Joaquin Basin, California. *Clays and Clay Minerals,* **34,** 115–124.

Reyes, A.G. (1990) Petrology of Philippine geothermal systems and the application of alteration mineralogy to their assessment. *Journal of Volcanology and Geothermal Research,* **43,** 279–309.

Šamajová, E., Kraus, I., and Mato, L. (1993) Origin of the clay minerals in hydrothermally altered volcanic rocks in the Kremnica ore district. In *Eleventh Conference on Clay Mineralogy and Petrology,* J. Konta, ed., Univerzita Karlova, Ceske Budejovice, Czech Republic, 37–46.

Schultz, L.G. (1964) *Quantitative Interpretation of Mineralogical Composition from X-ray and Chemical Data for the Pierre Shale.* US Geological Survey Professional Paper, Washington, D.C., 31 pp.

Scott, S.G. (1987) Stratigraphic coal drilling in the northern Bowen Basin. *Geological Survey of Queensland, Record 1987/53.*

Shaw, H.F. and Primmer, T.J. (1991) Diagenesis of mudrocks from the Kimmeridge Clay Formation of the Brae Area, UK North Sea. *Marine and Petroleum Geology,* **8,** 270–277.

Small, J.S. (1994) Fluid composition, mineralogy and morphological changes associated with the smectite-to-illite reaction: An experimental investigation of the effect of organic acid anions. *Clay Minerals,* **29,** 539–554.

Steiner, A. (1977) The Wairakei geothermal area, North Island, New Zealand. *New Zealand Geological Survey Bulletin 90,* Wellington, New Zealand, 136 pp.

Surdam, R.C. and Boles, J.R. (1979) Diagenesis of volcanic sandstones. In *Aspects of Diagenesis,* P.A. Scholle and P.S. Schluger, eds., Society of Economic Paleontologists and Mineralogists Special Publication 26, Tulsa, Oklahoma, 227–242.

Surdam, R., Crossey, L.J., Hagen, E.S., and Heasler, H.P. (1989) Organic-inorganic interactions and sandstone diagenesis. *American Association of Petroleum Geologists Bulletin,* **73,** 1–23.

Uysal, I.T. (1999) Mineralogy and isotope geochemistry of authigenic clay and carbonate minerals in Late Permian coal measures, Bowen Basin, Queensland: Implications for thermal and fluid flow history. Ph.D. thesis, University of Queensland, Brisbane, Australia, 253 pp.

Uysal, I.T., Glikson, M., Golding, S.D., and Audsley, F. (2000a) The thermal history of the Bowen Basin, Queensland, Australia: Vitrinite reflectance and clay mineralogy of the Late Permian coal measures. *Tectonophysics* (in press).

Uysal, I.T., Golding, S.D., and Thiede, D.S. (2000b) K-Ar and Rb-Sr dating of authigenic illite-smectite in Late Perm-

ian coal measures, Queensland, Australia: Implications for thermal history. *Chemical Geology* (in press).

Vavra, C.L. (1989) Mineral reactions and controls on zeolite-facies alteration in sandstone of the central Transantarctic Mountains, Antarctica. *Journal of Sedimentary Petrology,* **59,** 688–703.

Velde, B. and Vasseur, G. (1992) Estimation of the diagenetic smectite to illite transformation in time-temperature space. *American Mineralogist,* **77,** 967–976.

Welton, J.E. (1984) *SEM Petrology Atlas.* American Association of Petroleum Geologists, Tulsa, Oklahoma, 237 pp.

Whitney, G. (1990) Role of water in the smectite-to illite reaction. *Clays and Clay Minerals,* **38,** 343–350.

Whitney, G. and Northrop, H.R. (1987) Diagenesis and fluid flow in the San Juan Basin, New Mexico: Regional zonation in the mineralogy and stable isotope composition of clay minerals in sandstone. *American Journal of Science,* **287,** 353–382.

Whitney, G. and Velde, B. (1993) Changes in particle morphology during illitization: An experimental study. *Clays and Clay Minerals,* **41,** 209–218.

WoldeGabriel, G. and Goff, F. (1992) K/Ar dates of hydrothermal clays from core hole VC-2B, Valles Caldera, New Mexico and their relation to alteration in a large hydrothermal system. *Journal of Volcanology and Geothermal Research,* **50,** 207–230.

Yau, Y.C., Peacor, D.R., Essene, E.J., Lee, J.H., Kuo, L.C., and Cosca, M.A. (1987) Hydrothermal treatment of smectite, illite, and basalt to 460°C: Comparison of natural with hydrothermally formed clay minerals. *Clays and Clay Minerals,* **35,** 241–250.

Yau, Y.C., Peacor, D.R., Beane, R.E., Essene, E.J., and McDowell, S.D. (1988) Microstructures, formation mechanisms, and depth-zoning of phyllosilicates in geothermally altered shales, Salton Sea, California. *Clays and Clay Minerals,* **36,** 1–10.

Ylagan, R.F., Altaner, S.P, and Pozzuoli, A. (1996). Hydrothermal alteration of a rhyolitic hyaloclastite from Ponza Island, Italy. *Journal of Volcanology and Geothermal Research,* **74,** 215–231.

E-mail of corresponding author: t.uysal@earthsciences.uq.edu.au

(Received 24 June 1999; accepted 2 February 2000; Ms. 354; A.E. Stephen Altaner)